Brief Communications

Human Neuroma Contains Increased Levels of Semaphorin 3A, Which Surrounds Nerve Fibers and Reduces Neurite Extension *In Vitro*

Martijn R. Tannemaat,[1,2] Joanna Korecka,[1] Erich M. E. Ehlert,[1] Matthew R. J. Mason,[1] Sjoerd G. van Duinen,[3] Gerard J. Boer,[1] Martijn J. A. Malessy,[2] and Joost Verhaagen[1]

[1]Laboratory for Neuroregeneration, Netherlands Institute for Neuroscience, An Institute of the Royal Academy of Arts and Sciences, 1105 BA Amsterdam, The Netherlands, and [2]Department of Neurosurgery and [3]Department of Pathology and Neurology, Leiden University Medical Center, 2300 RC Leiden, The Netherlands

Neuroma formation after peripheral nerve injury is detrimental to functional recovery and is therefore a significant clinical problem. The molecular basis for this phenomenon is not fully understood. Here, we show that the expression of the chemorepulsive protein semaphorin 3A (sema3A), but not semaphorin 3F, is increased in human neuroma tissue that has formed in severe obstetric brachial plexus lesions. Sema3A is produced by fibroblasts in the epineurial space and appears to be secreted into the extracellular matrix. It surrounds fascicles, minifascicles, or single axons, suggesting a role in fasciculation and inhibition of neurite outgrowth. Lentiviral vector-mediated knock-down of Neuropilin 1, the receptor for sema3A, leads to increased neurite outgrowth of F11 cells cultured on neuroma tissue, but not of F11 cells cultured on normal nerve tissue. These findings demonstrate the putative inhibitory role of sema3A in human neuroma tissue. Our observations are the first demonstration of the expression of sema3A in human neural scar tissue and support a role for this protein in the inhibition of axonal regeneration in injured human peripheral nerves. These findings contribute to the understanding of the outgrowth inhibitory properties of neuroma tissue.

Key words: **semaphorin 3A; peripheral nerve; regeneration; inhibition; fasciculation; neuroma; brachial plexus**

Introduction

Severe peripheral nerve lesions can cause life-long functional impairments. A typical example is the obstetric brachial plexus injury that occurs in two to three of every 1000 births (Pondaag et al., 2004). Severe traction to the brachial plexus during birth induces the formation of intraneural scar tissue. This is known as "neuroma in continuity" (MacKinnon and Dellon, 1988) and constitutes an environment that inhibits nerve regeneration (Sunderland, 1991). Resection of the neuroma and bridging of the gap with autologous nerve grafts to connect proximal and distal nerve stumps usually results in some axonal regeneration, but functional recovery is never complete. Therefore, neuroma formation is a significant clinical problem.

The molecular basis for the outgrowth-inhibitory properties of neuromas is not fully understood (Sunderland, 1991), but may be partly caused by the excessive proliferation of fibroblasts which in turn produce inhibitory molecules (Badalamente et al., 1985; Morgenstern et al., 2003). A number of molecules have now been identified which are growth-inhibitory in the nervous system, for example, Nogo, chondroitin sulfate proteoglycans, and chemorepulsive axon guidance proteins (Fawcett, 2006). In the peripheral nerve neuroma, the secreted chemorepulsive axon guidance proteins semaphorins 3A (sema3A) and 3F (sema3F) may be of particular importance, for several reasons. First, their expression is upregulated in the rat sciatic nerve distal to a lesion (Scarlato et al., 2003; Ara et al., 2004). Second, the receptor for sema3A, neuropilin 1 (npn1), is constitutively expressed in motoneurons and sensory neurons of the peripheral nerve (Pasterkamp et al., 1998; Lindholm et al., 2004) and adult sensory neurons remain sensitive to sema3A (Reza et al., 1999; Tang et al., 2004). Finally, in the developing brachial plexus, sema3A and sema3F coordinate the timing and fasciculation of motor axon growth and determine the dorsoventral organization of motor axon projections (Huber et al., 2005).

We studied the expression of sema3A and sema3F in neuroma tissue from nine obstetric brachial plexus injury patients that was removed during reconstructive surgery. Tissue from the same nerve trunk proximal to the neuroma served as a control. A small segment of this proximal nerve stump is routinely harvested for intraoperative neuropathological assessment, as its quality influences surgical decision making (Malessy et al., 1999). The availability of this material provided us with the unique opportunity to compare, within a single nerve, two types of tissue with con-

Received April 26, 2007; accepted Nov. 2, 2007.

This work was partially supported by a grant from the Netherlands Brain Foundation (project number 15F07) (The Hague, The Netherlands), a grant from the Prinses Beatrix Fonds, a gift from S. Matser-van Nulck (Hilversum, The Netherlands), and a grant from the International Spinal Cord Research Trust (STR090). We thank B. Hobo for her assistance with the sema3A Western blot.

Correspondence should be addressed to Dr. Joost Verhaagen, Netherlands Institute for Neuroscience, Meibergdreef 47, 1105 BA Amsterdam ZO, The Netherlands. E-mail: j.verhaagen@nin.knaw.nl.

DOI:10.1523/JNEUROSCI.4571-07.2007

 0270-6474/07/2714260-05$15.00/0

trasting properties: the outgrowth-inhibitory environment of the neuroma and the outgrowth-supporting environment in the stump proximal to the neuroma.

Here, we show that the expression of sema3A, but not sema3F, is induced in fibroblasts present in neuroma tissue of obstetric injuries to the upper brachial plexus. Sema3A is localized around fascicles or around individual axons and inhibits the outgrowth of neurites from a neuronal cell line cultured on slices of human neuroma tissue. This is the first demonstration of the expression of this chemorepulsive protein in human neural scar tissue and the results point to a role for sema3A in the inhibition of axonal regeneration in injured human peripheral nerves.

Materials and Methods

Materials. The average age of patients was 5 months (range, 4–6 months). Nerve and neuroma material was harvested during reconstructive brachial plexus surgery, snap-frozen within 15 min after surgical removal, and stored at −80°C. All material used in this study was anonymized according to the proper use code of the Pathology Department of the Leiden University Medical Center. Neuroma material consisted of the upper branches of the brachial plexus: spinal nerve C6 ($n = 2$) or the superior trunk of the brachial plexus ($n = 7$). The proximal nerve stump consisted of a segment of the spinal nerve C5 ($n = 7$) or C6 ($n = 2$). All material was diagnosed intraoperatively as neuroma or as proximal nerve stump suitable for grafting according to previously described criteria (Malessy et al., 1999).

RNA isolation and qPCR. Tissue samples were homogenized in 3 ml of Trizol (Invitrogen, Eugene, OR) per 100 mg using an ultra-turrax device. After phase separation by addition of chloroform, the aqueous phase was mixed with an equal volume of 70% ethanol, further purified with an RNeasy Mini column (Qiagen, Valencia, CA) and stored at −80°C. The quality of the RNA was determined using a 2100 Bioanalyzer (Agilent, Palo Alto, CA). The average RNA integrity number was 8.2 (range, 6.4–9.3). cDNA was synthesized from 150 ng of RNA using Superscript II (Invitrogen). Real-time quantitative PCR (qPCR) on sema3A and sema3F expression was performed with SYBR-green master mix (Applied Biosystems, Foster City, CA) on an ABI5700 (Applied Biosystems) (Hope et al., 2003). Expression levels were normalized using the geometric mean of the three reference genes B2M (*beta-2-microglobulin*), YWHAZ (*tyrosine 3-monooxygenase/tryptophan 5-monooxygenase activation protein, zeta polypeptide*), and HMBS (*hydroxymethyl-bilane synthase*) (Vandesompele et al., 2002), which were selected from a total of six potential reference genes as being the most stably expressed genes in our samples. For a list of all primer sequences, see supplemental Table 1 (available at www.jneurosci.org as supplemental material).

In situ *hybridization.* A 590 base pair (bp) fragment ranging from bp 1726–2316 was cut from a plasmid containing the full-length human sema3A cDNA (Giger et al., 1998) with the restriction enzymes *Nco*I and *Hind*III and subcloned into pBluescript (Stratagene, La Jolla, CA). This region was selected for the construction of riboprobe because of its limited homology to other secreted semaphorins. Digoxigenin-labeled sense and antisense cRNA probes were made as described previously (Giger et al., 1998), but to increase binding specificity, alkaline hydrolysis of the probe was not performed, resulting in a probe length of 590 bp. *In situ* hybridization was performed on 10-μm-thick transverse cryostat sections as described previously (Mason et al., 2002) with a probe concentration of 600 ng/ml and a hybridization temperature of 67°C. The specificity of the hybridization signal was verified by comparison with the sections processed with sense probe under identical conditions.

Immunohistochemistry. Neuroma and proximal nerve stump samples were cut into transverse, 20-μm-thick cryostat sections and fixed in 4% paraformaldehyde in 0.1 M sodium phosphate buffer, pH 7.4, for 20 min. Immunohistochemistry was performed (De Wit et al., 2005) with the primary antibodies mouse anti-neurofilament (1:1000, 2H3 ascites; Developmental Studies Hybridoma Bank, University of Iowa, IA) to visualize neurites, rabbit anti-S100 (1:200; Dako, High Wycombe, UK) to visualize Schwann cells, and rabbit anti-fibronectin (1:100; Millipore, Temecula, CA) to visualize fibroblasts. To visualize sema3A, N15 goat anti-sema3A (1:25; Santa Cruz Biotechnology, Santa Cruz, CA), C17 goat anti-sema3A (1:25; Santa Cruz Biotechnology), and Q18 goat anti-sema3A (1:25; Santa Cruz Biotechnology) were used. These three sema3A antibodies bind to distinct epitopes in sema3A. N15 binds to an epitope that lies within a region corresponding to amino acids 25–75 of the human sema3A, C17 to a region corresponding to amino acids 721–771 and Q18 to an epitope corresponding to a region between amino acids 675–725 (for information on epitopes from manufacturers, see supplemental Fig. 1, available at www.jneurosci.org as supplemental material).

For neurofilament and S100/fibronectin, donkey anti-mouse-Cy3 and donkey anti-rabbit-Cy3 were used as secondary antibodies respectively (1:400; Jackson ImmunoReagents, West Grove, PA). For N15, C17, and Q18, biotinylated anti-goat antibody (1:800; Vector Laboratories) was used followed by streptavidin-Cy2 (1:800; Jackson ImmunoReagents).

Short-hairpin-mediated knock-down of npn1 *in a neuronal cell line.* F11 cells are derived from a fusion of mouse embryonic neuroblastoma cells and rat dorsal root ganglion neurons (Platika et al., 1985). Neurite outgrowth in these cells can be induced by withdrawal of serum and the addition of forskolin to the culture medium. To knock down the expression of *npn1* in F11 cells, they were transduced at a multiplicity of infection of 50 with a lentiviral (LV) vector expressing a short-hairpin (sh) RNA targeting the *npn1* sequence CTTCAACCCACATTTCGAT under an H1 promoter (Brummelkamp et al., 2002) next to a CMV promoter driving the expression of green fluorescent protein (GFP). As a control, F11 cells were transduced with an LV vector encoding an shRNA targeting the Arabidopsis sequence AGATCCTCTGTTCTCTCTC (which has no homology to mammalian genes). Knock-down of *npn1* was determined with qPCR as described above using primers and reference genes listed in supplemental Table 1 (available at www.jneurosci.org as supplemental material).

Culture of F11 cells on neuroma sections and quantification of neurite outgrowth. A total of 2.5×10^4 F11 cells, transduced with either *npn1* knock-down or control vector, were plated onto thawed 20-μm-thick cryostat sections of freshly frozen nerve or neuroma from five patients in 500 μl of DMEM containing 0.5% fetal bovine serum, 100 IU/ml penicillin, 100 μg/ml streptomycin, 2 mM Glutamax (Sigma, St. Louis, MO), and 20 μg/ml forskolin. After 48 h, cells were fixed in 4% paraformaldehyde in 0.1 M sodium phosphate buffer and coverslipped. For each condition, three standardized images of GFP positive F11 cells were randomly made using a Zeiss (Oberkochen, Germany) Axioplan 2 microscope and an Evolution QEi digital camera (MediaCybernetics, Silver Spring, MD). A total number of 1599 cells and their neurites were manually outlined by an observer blinded to the treatment using Image-Pro Plus software (version 5.1; MediaCybernetics) and the total neurite outgrowth per cell was calculated. The values for *npn1* knock-down or control cells were averaged for each nerve and neuroma ($n = 5$ in four groups) before statistical analysis.

Statistical analysis. All samples were tested for normality with a Shapiro-Wilk test. In cases where $W > 0.05$, a paired two-tailed Student's *t* test was performed, in all other cases a Wilcoxon signed-rank test was performed. A p value <0.05 was considered significant.

Results

Neural architecture

Neurofilament staining showed a difference in the cellular architecture of the proximal nerve stump and the neuroma (Fig. 1*a*). In the proximal nerve stump, axons aligned tightly within fascicles and were oriented perpendicular to the transverse section. The neuroma usually had a much larger cross-sectional area (Fig. 1*a*, insets), in which axons could be identified in fascicles, minifascicles or as single axons. Fascicles were oriented in different directions in a chaotic pattern within the epineurium.

qPCR

The expression levels of sema3A and sema3F as determined by qPCR and compared directly to the proximal nerve stump from the same patient showed a 1.8-fold higher level of sema3A in the

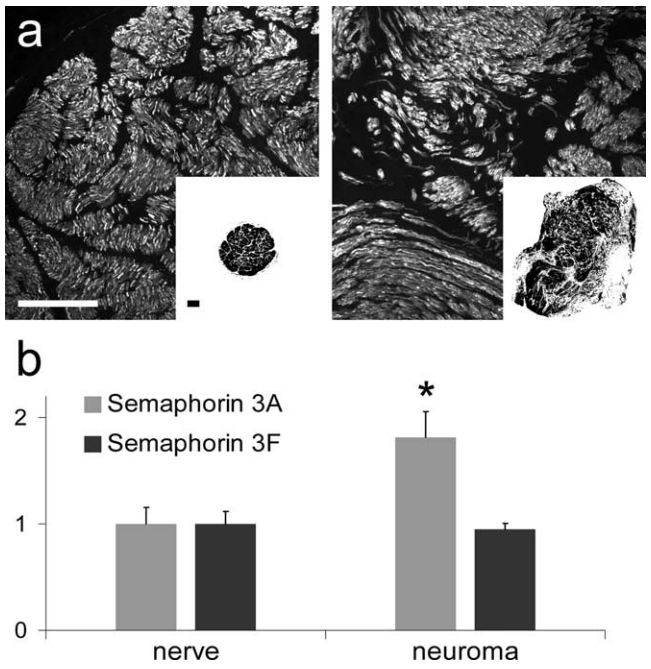

Figure 1. Structure of the proximal nerve stump and neuroma from the human brachial plexus and the expression of semaphorin 3A and 3F. ***a***, Neurofilament staining of cross-sections of the proximal nerve stump and the neuroma. In the nerve (left), compact fascicles contain high numbers of closely aligned nerve fibers. In the neuroma (right), nerve fibers are randomly oriented, grouped in either fascicles, minifascicles or as single fibers. Insets, Representative images of cross-sections of nerve and neuroma, showing that the neuroma is larger and more irregularly shaped than the nerve. Scale bar, 250 μm. ***b***, The average expression of sema3A as determined by qPCR is 1.8-fold higher in the neuroma than in the proximal nerve stump (*$p = 0.008$, Wilcoxon signed-rank test), whereas the expression of sema3F does not differ significantly. Error bars indicate the average ± SEM for $n = 9$.

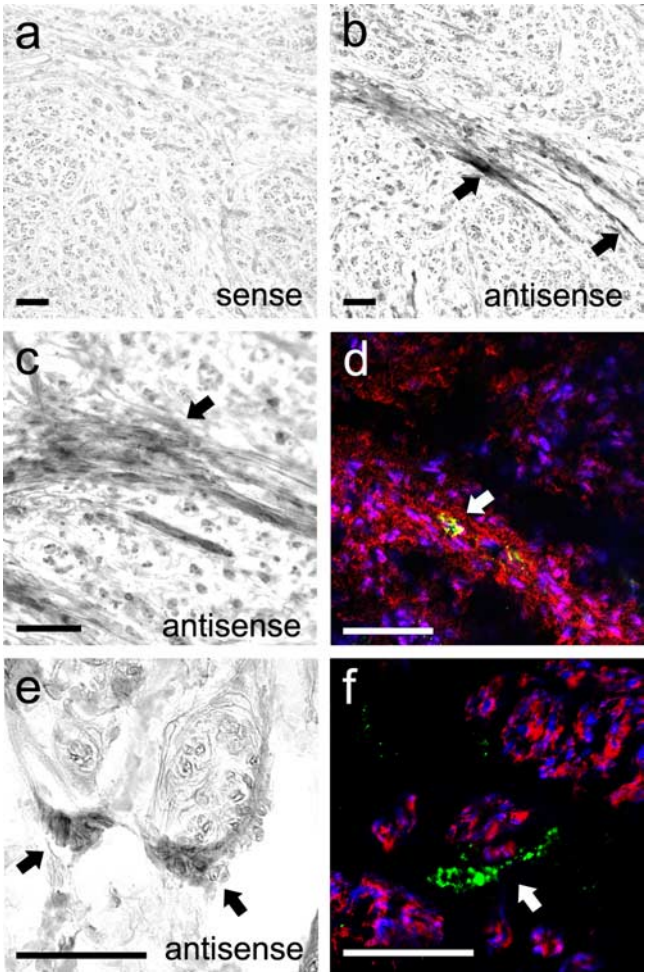

Figure 2. Extrafascicular fibroblasts are the primary source of sema3A. ***a***, *In situ* hybridization with the sense probe shows some staining of myelin that is also seen with the antisense probe, but the intense staining of extrafascicular cells is not present. ***b***, ***c***, ***e***, Hybridization with the antisense probe shows cells with a strong fibroblast-like morphology expressing *sema3A*. The highest expression levels are seen surrounding fascicles (***b***), between fascicles (***c***), and surrounding minifascicles (***e***). ***d***, Immune histology for fibronectin (red), sema3A (N15 antibody, green) and cell nuclei (blue): sema3A is present in fibronectin-rich areas between fascicles. ***f***, Immune histology for S100 (red), neurofilament (blue), and sema3A (green). S100-positive Schwann cells surround axons and do not colocalize with sema3A. The localization of the sema3A protein closely resembles the staining of sema3A mRNA obtained with *in situ* hybridization. The arrows point at areas of sema3A expression. Scale bars: 50 μm.

neuroma tissue ($p = 0.008$), whereas no difference was observed for sema3F (Fig. 1*b*).

In situ hybridization

In situ hybridization was performed to determine the cell type that expresses *sema3A* in the neuroma. Hybridization with the antisense sema3A probe resulted in strong staining of large epineurial and perineurial cells with a typical fibroblast-like morphology surrounding fascicles (Fig. 2*b*,c) or mini-fascicles (*e*). Both the antisense and the sense probe revealed some staining of other structures, particularly of myelinated axons (Fig. 2*a*,*b*). This was considered to be background staining and not the result of specific binding to sema3A mRNA.

Immunohistochemistry

Sema3A could be visualized with the N15 antibody in some proximal nerve stumps ($n = 4$), in which case it was almost always located in the epineurial space on the outer boundaries of the nerve (Fig. 3*a*) or in between fascicles. Very rarely, an area within a fascicle was weakly positive for sema3A (Fig. 3*b*). In contrast, sema3A staining could be seen in neuroma tissue from all nine patients and the intensity of sema3A staining was much higher than in proximal nerve stumps. It was present in a typical punctate pattern in small, defined areas within the section, apparently secreted into the extracellular matrix. In some neuromas sema3A was also present more diffusely between nerve fascicles (Fig. 3*c*). Sema3A was observed in close proximity to minifascicles (Fig. 3*c*,*e*,*f*) or single nerve fibers (Fig. 3*d*). Sema3A staining was not observed around all fascicles, but appeared to be present around a subset of nerve bundles. When a minifascicle was cut transversely, sema3A staining often appeared to surround the axon bundles (Fig. 3*f*). Three-dimensional reconstructions of *z*-stacked confocal images revealed an intimate relation between secreted sema3A and axons (supplemental Movie 1, available at www.jneurosci.org as supplemental material). Highly similar and overlapping staining patterns in adjacent sections were obtained with all three antibodies. For additional details on sema3A antibody specificity, see the supplemental material (available at www.jneurosci.org).

Immunohistochemistry for S100, neurofilament and sema3A (Fig. 2*e*) revealed S100 positive Schwann cells enveloping axons. No colocalization of S100 and sema3A was observed (Fig. 2*f*). Immunohistochemistry for fibronectin and sema3A showed that sema3A was primarily present in fibronectin-rich areas associated with perineurial fibroblasts (Fig. 2*d*), consistent with the expression of sema3A mRNA by fibroblast-like cells surrounding

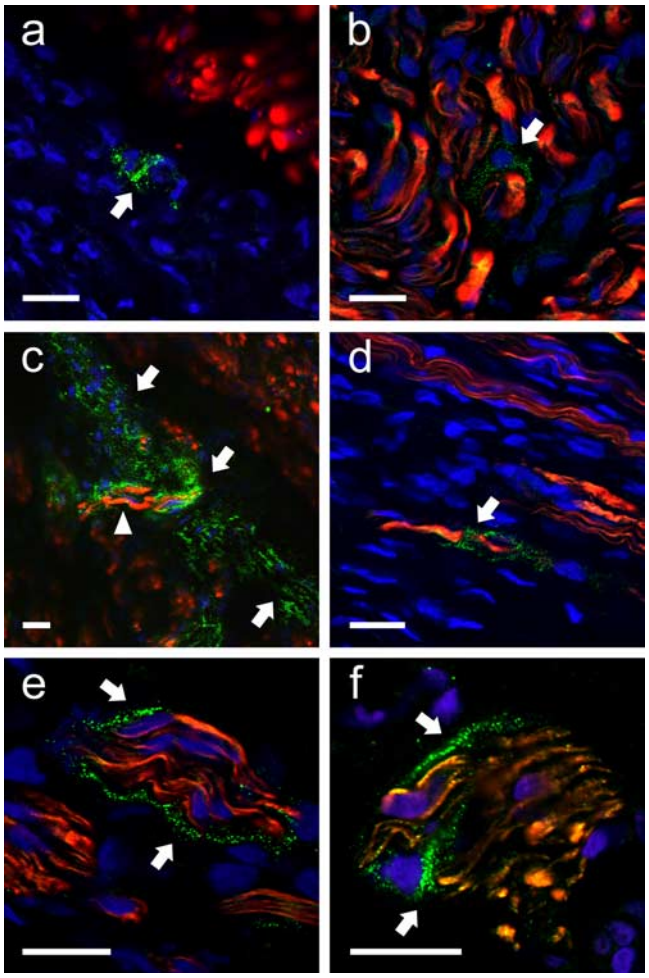

Figure 3. Immune histology for sema3A and neurofilament in the human proximal nerve stump and neuroma. Sema3A (N15 antibody, green), neurofilament (2H3 antibody; red) and cell nuclei (Topro; blue) are visualized. ***a***, Proximal nerve stump: sema3A expression was usually low and limited to the epineurium surrounding a fascicle. ***b***, Proximal nerve stump: rarely, a weak sema3A signal was observed within a fascicle. ***c***, Neuroma: sema3A is present in a diffuse pattern in the epineurial space in the neuroma, with the highest intensity of staining in the proximity of a minifascicle (arrowhead). ***d***, Neuroma: sema3A surrounds a single axon. ***e***, ***f***, Neuroma: sema3A surrounds a minifascicle. A three-dimensional projection of a *z*-stack of Figure 2*e* is available at www.jneurosci.org as supplemental material. The arrows point at areas of sema3A expression, and the arrowhead points at a minifascicle. Scale bars: 20 μm.

nerve fascicles (Fig. 2). These observations demonstrate that fibroblasts are the primary source of sema3A in the neuroma.

Neurite outgrowth assay

F11 cells plated on neuroma sections displayed significantly less outgrowth compared with F11 cells plated on nerve sections (60 vs 83 μm; $p < 0.05$) (Fig. 4*b*). LV-mediated expression of an shRNA targeting *npn1* resulted in a knock-down of 77% of *npn1* expression. Knock-down of *npn1* did not affect neurite length of F11 cells grown on nerve sections ($p = 0.69$). In contrast, on neuroma sections the total neurite outgrowth per cell was increased for cells with a knock-down of *npn1* expression (101 vs 60 μm; $p < 0.01$) (Fig. 4*b*). LV vector-mediated knock-down of *npn1* thus leads to increased neurite outgrowth of F11 cells when plated on neuroma tissue, but not when plated on nerve tissue. This indicates that in the neuroma, sema3A has a chemorepulsive effect on growing neurites.

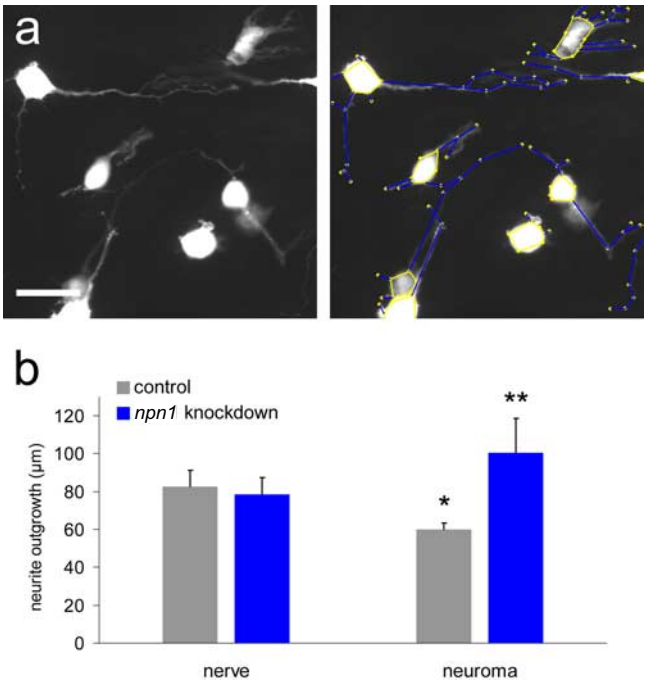

Figure 4. Neurite outgrowth of F11 cells is inhibited on neuroma sections *in vitro*. Knock-down of *npn1* increases neurite outgrowth on neuroma, but not on normal nerve tissue. ***a***, Left, F11 cells cultured on neuroma tissue for 48 h. Most F11 cells extend at least one neurite. Right, Cells (yellow lines) and neurites (blue lines) were manually outlined by an observer blinded to the treatment. Scale bar, 50 μm. ***b***, Quantification of outgrowth. Neurite outgrowth of wild-type F11 cells is inhibited on neuroma tissue compared with control F11 cells on nerve tissue (*$p < 0.05$, paired two-tailed Student's *t* test). Knock-down of npn1 leads to an increase in neurite outgrowth per cell on neuroma tissue (**$p < 0.01$, paired two-tailed Student's *t* test), but has no effect on the neurite outgrowth of F11 cells grown on normal nerve tissue.

Discussion

It is widely accepted that neuroma formation at the site of a human peripheral nerve lesion is deleterious to functional recovery. Little is known, however, about the molecular basis for this phenomenon (Sunderland, 1991). In this study, we show for the first time that several months after the initial trauma the secreted chemorepulsive sema3A is present in human neuroma tissue.

Sema3A is expressed by epineurial and perineurial fibroblasts, but not by Schwann cells. Lesion-induced upregulation of class 3 semaphorins was first noted in meningeal fibroblasts that form the core of the neural scar after penetrating CNS injuries in a rat model (Pasterkamp et al., 1999; de Winter et al., 2002). Sema3A is also induced in epineurial and perineurial fibroblasts distal to a rat peripheral nerve lesion (Scarlato et al. 2003). These observations suggest that the activation of fibroblasts at lesion sites in both the CNS and PNS results in enhanced expression of inhibitory proteins like sema3A.

Sema3A protein appears to be secreted by fibroblasts and surrounds neurites and fascicles in a punctate pattern typical for extracellular matrix proteins (De Wit et al., 2005, 2006). The close proximity of sema3A to axons and its neurite outgrowth-inhibitory effect on F11 cells suggest that sema3A contributes to the fasciculation of regenerating neurites through a mechanism of "surround repulsion," similar to what has been observed during development (Huber et al., 2005). Secreted sema3A binds to extracellular chondroitin sulfate proteoglycans (CSPGs) *in vitro* (De Wit et al., 2005). CSPGs (Snow et al., 2003) and peripheral nerve-derived fibroblasts (Morgenstern et al., 2003) induce fasciculation *in vitro*. A possible interaction between secreted sema-

phorins and CSPGs may therefore stimulate fasciculation in the neuroma.

We propose that a severe traction injury to the brachial plexus causes a disruption of the normal architecture of the nerve and leads to proliferation and redistribution of fibroblasts from the epineurial and perineurial sheets within the nerve. During the process of neuroma formation sema3A is expressed by fibroblasts. In less severe nerve injuries, this may prevent regenerating axons from growing into epineurial tissue and thereby guide them toward the distal endoneurial tubes. There, Schwann cells produce a wide range of neurotrophic factors (Frostick et al., 1998), eventually leading to successful regeneration. The neuroma material used in this study, however, was obtained from patients without clinical signs of spontaneous functional recovery. This suggests that in these severe lesions, the proliferation of sema3A-secreting fibroblasts contributes to an environment that is hostile to regenerating fibers and counteracts the outgrowth-enhancing effects of the more distally located Schwann cells, leading to trapping of neurites within the fibrous scar. Previously, a naturally occurring small molecule was discovered that antagonizes sema3A and promotes recovery of function in a rat model of spinal cord injury (Kaneko et al., 2006). Progress in creating an animal model for the peripheral nerve neuroma (Sinis et al., 2007) will allow future studies on the effect of this compound on axonal regeneration through neuroma tissue. Such studies could lead to novel strategies that may be applied as an adjuvant therapy to peripheral nerve surgery.

References

Ara J, Bannerman P, Hahn A, Ramirez S, Pleasure D (2004) Modulation of sciatic nerve expression of class 3 semaphorins by nerve injury. Neurochem Res 29:1153–1159.

Badalamente MA, Hurst LC, Ellstein J, McDevitt CA (1985) The pathobiology of human neuromas: an electron microscopic and biochemical study. J Hand Surg [Br] 10:49–53.

Brummelkamp TR, Bernards R, Agami R (2002) A system for stable expression of short interfering RNAs in mammalian cells. Science 296:550–553.

De Winter F, Oudega M, Lankhorst AJ, Hamers FP, Blits B, Ruitenberg MJ, Pasterkamp RJ, Gispen WH, Verhaagen J (2002) Injury-induced class 3 semaphorin expression in the rat spinal cord. Exp Neurol 175:61–75.

De Wit J, De Winter F, Klooster J, Verhaagen J (2005) Semaphorin 3A displays a punctate distribution on the surface of neuronal cells and interacts with proteoglycans in the extracellular matrix. Mol Cell Neurosci 29:40–55.

De Wit J, Toonen RF, Verhaagen J, Verhage M (2006) Vesicular trafficking of semaphorin 3A is activity-dependent and differs between axons and dendrites. Traffic 7:1060–1077.

Fawcett JW (2006) Overcoming inhibition in the damaged spinal cord. J Neurotrauma 23:371–383.

Frostick SP, Yin Q, Kemp GJ (1998) Schwann cells, neurotrophic factors, and peripheral nerve regeneration. Microsurgery 18:397–405.

Giger RJ, Pasterkamp RJ, Heijnen S, Holtmaat AJ, Verhaagen J (1998) Anatomical distribution of the chemorepellent semaphorin III/collapsin-1 in the adult rat and human brain: predominant expression in structures of the olfactory-hippocampal pathway and the motor system. J Neurosci Res 52:27–42.

Hope AD, De Silva R, Fischer DF, Hol EM, Van Leeuwen FW, Lees AJ (2003) Alzheimer's associated variant ubiquitin causes inhibition of the 26S proteasome and chaperone expression. J Neurochem 86:394–404.

Huber AB, Kania A, Tran TS, Gu C, De Marco Garcia N, Lieberam I, Johnson D, Jessell TM, Ginty DD, Kolodkin AL (2005) Distinct roles for secreted semaphorin signaling in spinal motor axon guidance. Neuron 48:949–964.

Kaneko S, Iwanami A, Nakamura M, Kishino A, Kikuchi K, Shibata S, Okano HJ, Ikegami T, Moriya A, Konishi O, Nakayama C, Kumagai K, Kimura T, Sato Y, Goshima Y, Taniguchi M, Ito M, He Z, Toyama Y, Okano H (2006) A selective Sema3A inhibitor enhances regenerative responses and functional recovery of the injured spinal cord. Nat Med 12:1380–1389.

Lindholm T, Skold MK, Suneson A, Carlstedt T, Cullheim S, Risling M (2004) Semaphorin and neuropilin expression in motoneurons after intraspinal motoneuron axotomy. NeuroReport 15:649–654.

MacKinnon SE, Dellon AL (1988) Surgery of the peripheral nerve. New York: Thieme Medical.

Malessy MJ, van Duinen SG, Feirabend HK, Thomeer RT (1999) Correlation between histopathological findings in C-5 and C-6 nerve stumps and motor recovery following nerve grafting for repair of brachial plexus injury. J Neurosurg 91:636–644.

Mason MR, Lieberman AR, Grenningloh G, Anderson PN (2002) Transcriptional upregulation of SCG10 and CAP-23 is correlated with regeneration of the axons of peripheral and central neurons in vivo. Mol Cell Neurosci 20:595–615.

Morgenstern DA, Asher RA, Naidu M, Carlstedt T, Levine JM, Fawcett JW (2003) Expression and glycanation of the NG2 proteoglycan in developing, adult, and damaged peripheral nerve. Mol Cell Neurosci 24:787–802.

Pasterkamp RJ, Giger RJ, Verhaagen J (1998) Regulation of semaphorin III/collapsin-1 gene expression during peripheral nerve regeneration. Exp Neurol 153:313–327.

Pasterkamp RJ, Giger RJ, Ruitenberg MJ, Holtmaat AJ, De Wit J, De Winter F, Verhaagen J (1999) Expression of the gene encoding the chemorepellent semaphorin III is induced in the fibroblast component of neural scar tissue formed following injuries of adult but not neonatal CNS. Mol Cell Neurosci 13:143–166.

Platika D, Boulos MH, Baizer L, Fishman MC (1985) Neuronal traits of clonal cell lines derived by fusion of dorsal root ganglia neurons with neuroblastoma cells. Proc Natl Acad Sci USA 82:3499–3503.

Pondaag W, Malessy MJ, van Dijk JG, Thomeer RT (2004) Natural history of obstetric brachial plexus palsy: a systematic review. Dev Med Child Neurol 46:138–144.

Reza JN, Gavazzi I, Cohen J (1999) Neuropilin-1 is expressed on adult mammalian dorsal root ganglion neurons and mediates semaphorin3a/collapsin-1-induced growth cone collapse by small diameter sensory afferents. Mol Cell Neurosci 14:317–326.

Scarlato M, Ara J, Bannerman P, Scherer S, Pleasure D (2003) Induction of neuropilins-1 and -2 and their ligands, Sema3A, Sema3F, and VEGF, during Wallerian degeneration in the peripheral nervous system. Exp Neurol 183:489–498.

Sinis N, Haerle M, Becker ST, Schulte-Eversum C, Vonthein R, Rosner H, Schaller HE (2007) Neuroma formation in a rat median nerve model: influence of distal stump and muscular coating. Plast Reconstr Surg 119:960–966.

Snow DM, Smith JD, Cunningham AT, McFarlin J, Goshorn EC (2003) Neurite elongation on chondroitin sulfate proteoglycans is characterized by axonal fasciculation. Exp Neurol 182:310–321.

Sunderland S (1991) Nerve injuries and their repair: a critical appraisal. Melbourne: Chuchill Livingstone.

Tang XQ, Tanelian DL, Smith GM (2004) Semaphorin3A inhibits nerve growth factor-induced sprouting of nociceptive afferents in adult rat spinal cord. J Neurosci 24:819–827.

Vandesompele J, De Preter K, Pattyn F, Poppe B, Van Roy N, De Paepe A, Speleman F (2002) Accurate normalization of real-time quantitative RT-PCR data by geometric averaging of multiple internal control genes. Genome Biol 3:RESEARCH0034.